*Met. Mater. Int., Vol. 23, No. 5 (2017), pp. 1019~1028*
doi: 10.1007/s12540-017-6760-3

# Microstructure and Homogeneity of Semi-Solid 7075 Aluminum Tubes Processed by Parallel Tubular Channel Angular Pressing

**Ramin Meshkabadi[1], Ghader Faraji[1,*], Akbar Javdani[2], Ali Fata[1], and Vahid Pouyafar[2]**

[1]School of Mechanical Engineering, College of Engineering, University of Tehran, Tehran 11155-4563, Iran
[2]Department of Mechanical Engineering, University of Tabriz, 29 Bahman Blvd., Tabriz 5166616471, Iran

(received date: 24 October 2016 / accepted date: 17 February 2016)

Semi-solid processing is a new developing technology for the fabrication of intricate parts at low temperatures in comparison with conventional casting routes. In this research, a parallel tubular channel angular pressing (PTCAP) was used as a pre strain-inducing process, and the influence of the number of PTCAP passes and semi-solid heating parameters on the microstructural characteristics of Al7075 tubes was investigated. The results demonstrated that PTCAP process could successfully be used as a best pre-straining method for tubular samples showing semi-solid microstructures. As the temperature is increased, the solid particle size first decreased, then increased, and gradually became more spherical. The appropriate condition for the subsequent semi-solid forming process was gained at reheating temperature of 620 $^{0}$C. The suitability of this temperature was confirmed by the uniform distribution of grains. The grain size and shape factor both increased along with increasing the holding time. The distribution of the solid particles was strongly dependent upon the holding time and became uniform as the holding time increased. Comparison of the grain size and shape factor between ECAPed and PTCAPed samples revealed a high capacity of the PTCAP process as a strain-inducing stage. Also the two-pass PTCAP samples exhibited higher hardness than one-pass treated samples in the semi-solid state.

**Keywords:** semi-solid forming, parallel tubular channel angular pressing, grain size, shape factor, grain size distribution, 7075 aluminum alloy

## 1. INTRODUCTION

Semi-solid processing is a forming technique for the fabrication of intricate parts using lower forming loads at a low temperature in comparison with conventional casting routes [1]. Billet preparation, reheating to a semi-solid state, and semi-solid forming are three major steps of semi-solid forming. Spherical solid particles dispersed within the liquid phase provides the advantages above. Preparation of initial feedstock with non-dendritic microstructures is an essential step in semi-solid forming [2]. Many Globulization routes [3] such as mechanical stir casting [4,5], electromagnetic stir casting [6], grain refining [7], mechanical or ultrasonic vibrations [8], cold deformation followed by controlled melting, such as strain-induced and melt activated (SIMA) [9] or recrystallization and partial remelting (RAP) [10-14], or even spray-casting [13,15] were proposed to produce non-dendritic structures. Among these routes SIMA or RAP present an entirely globular structure in the semi-solid state [9-15]. In a SIMA process, (a) a strain is induced to as-received alloy using deformation techniques, (b) the deformed alloy is reheated to the semi-solid state, and is held isothermally, and finally and (c) thixotropic forming occurs.

Top-down approaches like severe plastic deformation (SPD) processes are mostly used to supply initial fine-grained alloys for the SIMA process [2]. Different SPD methods have been widely utilized in the production of ultra-fine grained (UFG) structures in the form of bulk, sheet, and tubular materials [16]. In these processes, as-received metal experiences severe plastic deformation, in which high plastic strain values are imposed. In comparison with conventional metal forming methods, SPD offers advantages such as relatively unchanged cross section and better strain homogeneity [17,18]. Moreover, some case studies were reported on the application of SPD processes for bulk materials [19-23]. The need for tubes with excellent mechanical properties, having bulk materials with industrial applications has drawn researchers' attention toward using SPD processes for tubular components [24]. A comprehensive review of UFG tubes reported by Faraji and Kim [25] covers the last works in this field. These include equal channel angular pressing (ECAP) for hollow parts [26], tubular channel angular pressing (TCAP) [16], PTCAP [24], combined PTCAP [27], cyclic flaring and sinking [28], other

*Corresponding author: ghfaraji@ut.ac.ir

combined processes [29,30], high-pressure tube twisting [31], tube high pressure shearing [32], accumulative spin bonding [33], tube cyclic extrusion-compression [34], and tube cyclic expansion-extrusion [35].

7075 Aluminum alloy, as a high strength alloy having light weight with high usage in particular applications, has some features comparable to those of soft steel [36]. These lay the foundations for this alloy to be an excellent substitute for steel because of its higher strength to weight. Semi-solid forming of this alloy is almost necessary as it is usually shaped through a costly machining process because of its relatively lower ductility in metal forming methods. Numerous investigations have been conducted to achieve a spherical microstructure of this alloy for semi-solid forming. Hassas-Irani *et al.* [37] investigated about the effects of SIMA process parameters on the microstructure evolution of an A356 aluminum alloy. They obtained a fine uniform spherical microstructure by heating the pre-deformed specimen up to 45% at 615 °C for 6 min. Binesh and Aghaie-Khafri [38] studied the microstructural and mechanical behaviors of semi-solid 7075 aluminum alloy produced by SIMA method. They reported that using the cold compression process, followed by a semi-solid heating causes some phase evolutions that are appropriate to get a globular microstructure for the subsequent forming process. Mohammadi *et al.* [39] obtained a suitable feedstock for semi-solid forming by using the RAP method for 7075 aluminum alloy. They revealed that at a longer holding time, the globular grains coarsened slightly and the average grain sizes were increased. Bolouri *et al.* [40,41] investigated the effects of compression rates on the microstructure evolution of a semi-solid 7075 aluminum alloy produced by the SIMA process. The samples were deformed at ambient temperature by compression to an extent of up to 40% reduction. Their results showed that the average grain size was reduced gradually as the compression rate was being increased. Jiang *et al.* [42] analyzed the effects of isothermal temperature and soaking time on the microstructure of fabricated 7075 aluminum parts by SIMA and RAP methods. The RAP method had a more spherical microstructure, but a slightly larger grain size, as compared to the SIMA method. Some other studies have used ECAP as a strain-inducing step in SIMA method. Ashouri *et al.* [43] used the ECAP process for one to four passes to examine the effects of strain on the morphology and shape factor of reheated A356 alloy. Nedjad *et al.* [44] demonstrated that a combination of equal channel angular pressing and isothermal heating in the semi-solid state gives a semi-solid billet with spheroidal solid phase. Jiang *et al.* [45] investigated the microstructural evolution of AZ61 magnesium alloy deformed by ECAP during a semi-solid isothermal treatment. The results show that extrusion pass, isothermal temperature, and the processing route influence the microstructural evolutions of the alloy during the semi-solid isothermal treatment.

Obtaining spherical microstructure consisting of a solid phase dispersed in the liquid phase is a prerequisite for any semi-solid forming process. Achieving such a microstructure for tubular parts has not been reported so far in the literature though there is a broad range of demand in industries for tubular samples. The application of PTCAP as a strain-inducing stage in the SIMA process for producing severely deformed tubes and then the microstructural evaluation of the part in the semi-solid state are the main subjects of this investigation. This is important because some forming processes like radial forward tube extrusion, radial backward tube extrusion, and conventional seamless tube extrusion are performed on the tube-shaped raw materials [46]. In this article, the microstructural evolution of PTCAP-treated tubes in the semi-solid state is evaluated to determine the suitable parameters for the subsequent forming process. In this regard, by studying the effects of process parameters such as the number of passes, reheating temperature and time, the appropriate conditions for achieving a microstructure with suitable grain size and shape factor were determined. Also, the homogeneity of the microstructure and grain size distribution were discussed. This microstructure for tubular parts is a key point in producing large and complicated parts while using the benefits of semi-solid forming such as reduced production stages and low process loads.

## 2. EXPERIMENTAL PROCEDURE

The chemical composition of as-received 7075 aluminum alloy is shown in Table 1. Recently, Faraji *et al.* [24,47] introduced a PTCAP process as a method of imposing a large amounts of strain to the cylindrical tubes without changing the dimensions. In the present study, this new SPD method is used to impose deformation on the tubular samples in the first stage of the SIMA process. In this process, in the first half of the cycle, the tube is placed between the die and mandrel, and it is squeezed by the first punch (Fig. 1(a)). As the sample passes through the symmetric shear zone, the diameter of the tube increases and reaches to a maximum value. In the second half of the cycle, another punch returns the tube back to the initial diameter over the same shear zone as depicted in Fig. 1(b) [48].

The as-received samples were machined to an outer diameter of 20 mm, an inner diameter of 15 mm, and a length of 40 mm. The prepared tubes were subjected to one and two passes of PTCAP process at a room temperature. The pressing speed was 10 mm/min, and to reduce friction between the die and sample during the process, an $MoS_2$ spray was employed as a lubricant [49,50].

A PID-controlled resistance furnace was used to heat the

**Table 1.** Chemical composition of Al 7075 (mass fraction, %)

| Si | Fe | Mn | Cr | Cu | Mg | Zn | Al |
|---|---|---|---|---|---|---|---|
| 0.333 | 0.405 | 0.139 | 0.229 | 1.51 | 2.25 | 5.27 | Base |

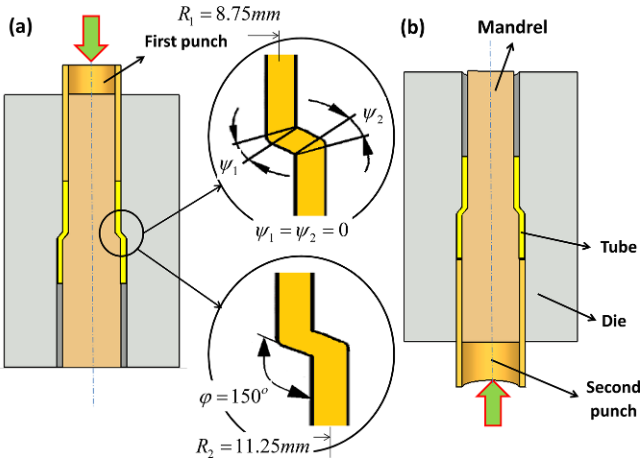


**Fig. 1.** Schematic representation of (a) the first and (b) the second half cycles of the PTCAP process [49].

samples, and a K-type thermometer system monitored the temperature of the slug. Since the heating time in the present study is short, we should consider the required time to reach a steady-state temperature. Thus, the heating curve of the sample was recorded. The average heating rate of the sample was 150 °C/min, and the temperature reached a semi-solid zone after about 4 minutes added to the holding time.

After heating the PTCAP-treated samples to predetermined temperatures of 610, 615, 620, and 625 °C and holding for a required time (5 min, 10 min, and 15 min), they were quenched in cold water. According to the DSC curve of this alloy, the corresponding values of the liquid fraction at these temperatures are 25%, 30%, 40%, and 50% [41].

To investigate the microstructure, the cross sections of the samples were polished and then etched using Keller's solution. The microstructures were observed using an optical microscope (OM). An image analysis software was used to determine the grain size ($d$) and shape factor (SF) of the microstructures using Eqs. (1) and (2):

$$d = \frac{\Sigma_1^N \sqrt{4A/\pi}}{N} \tag{1}$$

$$SF = \frac{1}{(\Sigma_1^N P^2/4\pi A)/N} \tag{2}$$

Where, $A$ is the surface area, $P$ is the perimeter, and $N$ is the number of particles in the selected area of the images [51]. To study the influence of input parameters on the mechanical properties of the deformed samples in the semi-solid state, hardness of the samples was measured.

## 3. RESULTS AND DISCUSSION

The optical micrograph of the 7075 aluminum alloy in the as-received condition is depicted in Fig. 2(a). The microstructure includes uncrystallized grains and dispersed intermetallic particles. Fig. 2(b) shows a picture of the PTCAP processed tubes after one or two passes.

### 3.1. The effect of number of PTCAP passes

Figure 3 shows the optical microstructures of the experimental alloy subjected to PTCAP for one and two passes, followed by heating at 610 °C for 5 min, 10 min, and 15 min. As is seen in Figs. 3(a) and 3(b), the solid phase is neither spherical nor fully isolated by a continuous liquid when processed for one and two passes held for 5 min at 610 °C. In this condition, as a result of lower reheating time, the liquid content is low, and it is mostly located along the grain boundaries [39]. The liquid phase has had an insufficient time to enter into the grain boundaries. Thus, the distribution of grains in the microstructure was non-uniform, and grain boundaries were discontinuous. This observation was not seen for 10 min and 15 min holding times. The one pass PTCAP possessed sample has a non-dendritic microstructure after reheating at

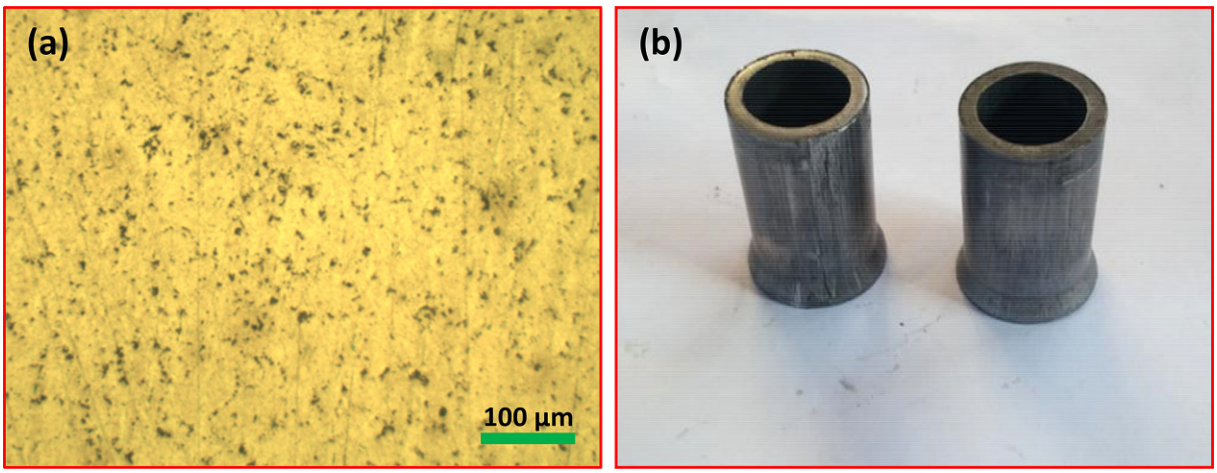


**Fig. 2.** (a) Microstructure of the alloy in as-received condition and (b) one and two pass treated tubes.

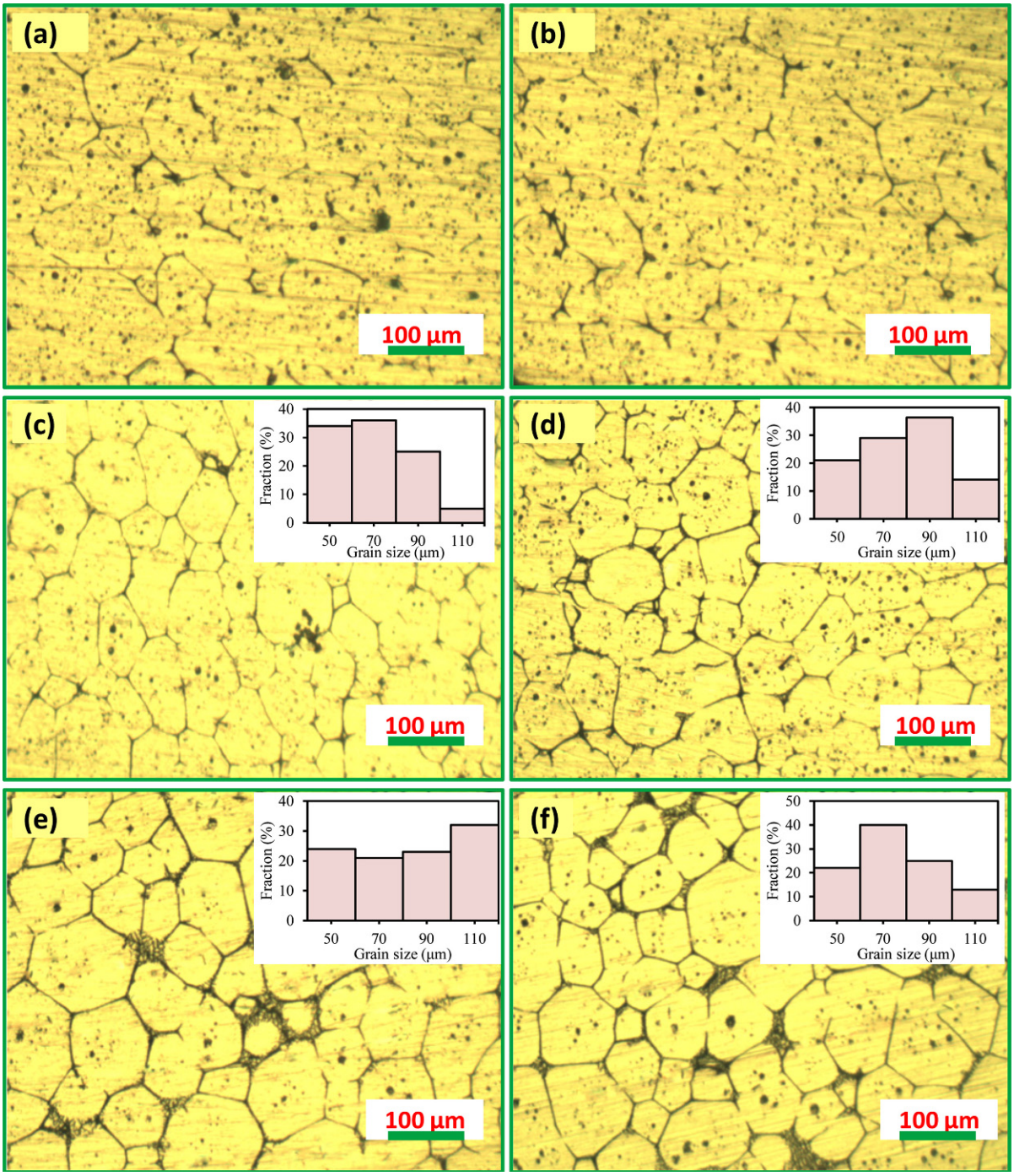


**Fig. 3.** Microstructures of the PTCAP-treated alloy held at 610 °C in different conditions; (a) 1-pass 5 min, (b) 2-passes 5 min, (c) 1-pass 10 min, (d) 2-passes 10 min, (e) 1-pass 15 min, and (f) 2-passes 15 min.

610 °C for 10 min and 15 min (Fig. 3(c) and 3(e)). In contrast, after applying the second pass PTCAP process, a prevailing spherical microstructure including rounded and disconnected solid particles has been formed, as shown in Fig. 3(d) and 3(f). The grain size and shape factor of the solid phase, as a function of the number of PTCAP passes, were plotted in Fig. 4. As is seen, increasing the number of PTCAP passes did not change the size of grains significantly, and only minor changes were observed in the shape factor.

After applying a one pass PTCAP process, the dislocation density increased as a result of a distortion in the crystal lattice. Next, the strain energy was stored as dislocation multiplication, elasticity stress, and vacancies which provided the driving force for recovery and recrystallization [52,53]. When

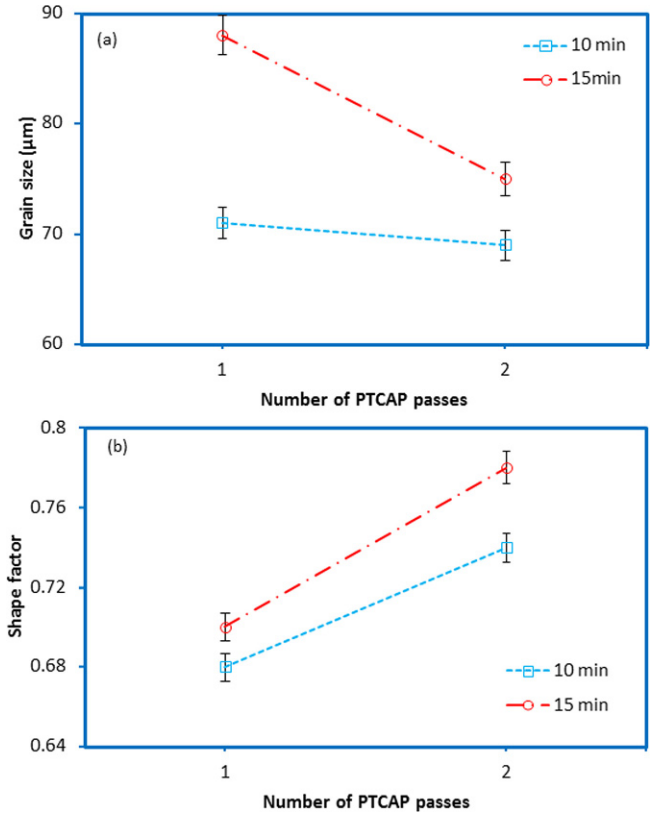


**Fig. 4.** Variations of (a) grain size and (b) shape factor with the number of the PTCAP pass after reheating at 610 °C for 10 min and 15 min.

the sample is heated at a semi-solid temperature and held for a specified duration, the stored strain energy was sufficient for recrystallization and growth of the solid phase along with the entrance of the liquid phase at the grain boundaries. When the liquid phase is formed, grain globularization and coarsening were activated simultaneously [53]. Increasing the number of PTCAP passes causes strain energy make greater in the material. However, it is not necessary for this process because it does not have a considerable impact on both the grain size and the shape factor. This recommends that one pass PTCAP can produce the favorable microstructure for consequent industrial applications. Though, the higher imposed strains may increase the dislocation density, and by that, it would turn into an entirely globular microstructure [37]. Accordingly, a little improvement of the shape factor in the two-pass PTCAP-treated specimen (Fig. 4(b)) is associated with the atomic diffusion rate as a result of higher dislocation density.

The histograms of the grain size distribution for the PTCAP-treated specimen in different numbers of passes, heating temperatures, and times were presented in Fig. 3. It could be seen from the histograms that one passed samples are not homogeneous in comparison with second pass processed ones. As the number of passes is increased, we could only achieve a uniform distribution, though the size of grains did not change significantly.

### 3.2. The effect of reheating temperature

Figure 5 illustrates the optical microstructures of the specimens pre-deformed by PTCAP through second passes and held at different temperatures of 610 °C, 615 °C, 620 °C, and 625 °C for 10 min. According to Figs. 5(a)-5(c), with increasing isothermal temperature from 610 °C to 620 °C, the liquid phase increases, and the grain size decreases. Also, the morphology of the solid grains becomes more globular. Some fine dendritic areas shown by red dashed lines in Fig. 5(d) are observed after reheating at 625 °C. Most of these dendritic areas are observed over the coarse grains. As the temperature increases to 625 °C, some solid particles begin melting and re-solidifying as fine dendrites (Fig. 5(d)) [37].

One of the principal mechanisms of grain coarsening is the coalescence of grains. Coalescence is typically characterized by the formation of one large grain consequent to the connection of two smaller ones. This mechanism, which occurs by grain boundary movement, is dominant at a low liquid fraction and short times [54]. As the liquid fraction increases, it is hard for the adjacent grains to coalesce continuously. Under these situations, Ostwald ripening is the prevailing mechanism of coarsening as a result of the high liquid fraction. Another coarsening mechanism which deals with the growth of large grains and loss of small ones is Ostwald ripening [54]. In this mechanism, grains continuously coarsen, and the small grains gradually melt [52,55,56]. The two mentioned mechanisms operate simultaneously and individually, once the liquid is formed [52].

Figure 6 shows the influence of reheating temperature on the average grain size and shape factor of the solid particles. From Fig. 6, it is clear that with an increase in the temperature, the size of solid grains decreases, and then it increases. This is attributed to the competing of coarsening and melting in the semi-solid state for increasing the grain size [57]. At the beginning of remelting, by increasing the temperature, the melting overcame the coarsening process and most of the solid grains are dissolved into the liquid phase, resulting in the reduction of the grain size [57]. Increasing temperature from 620 °C to 625 °C increases the grain size. Evaluation of the microstructures in Fig. 5 indicated that along with increasing temperature to 625 °C, ripening mechanisms have influenced the average size of the solid grains. The solid grains simply become spherical because of the effect of interface curvatures [39].

It can be seen from Fig. 6 that the solid grains gradually became more globular as the temperature increases from 610 °C to 625 °C. As is well known, an ideal microstructure for semi-solid forming includes grains smaller than 100 µm and shape factors greater than 0.7 [58,59]. Moreover, obtained results from Fig. 6 clearly indicate that the appropriate condition for the subsequent semi-solid forming process could be

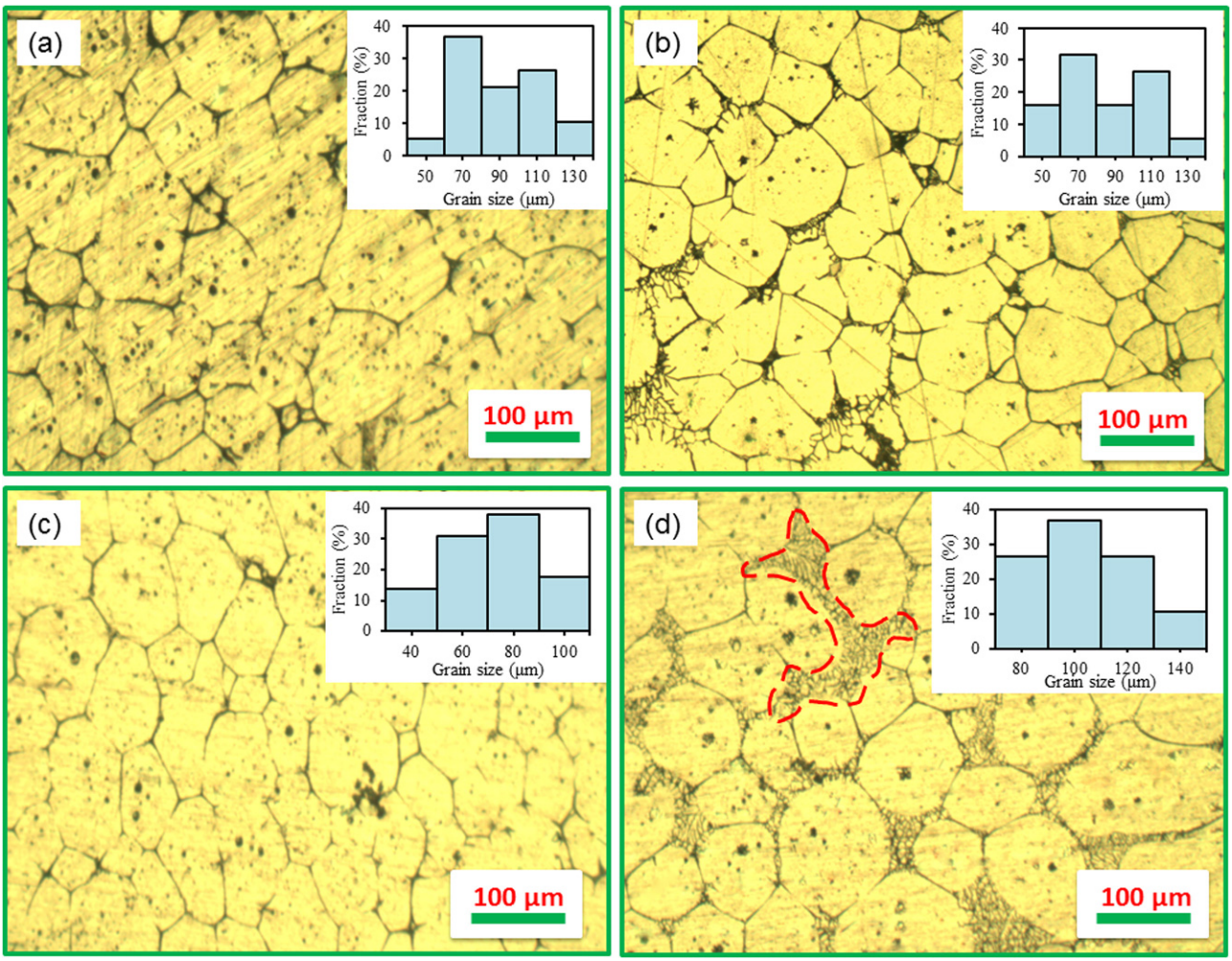


**Fig. 5.** Microstructure of the two-pass PTCAP-treated samples after reheating at different temperatures of (a) 610 °C, (b) 615 °C, (c) 620 °C and (d) 625 °C for 10 min.

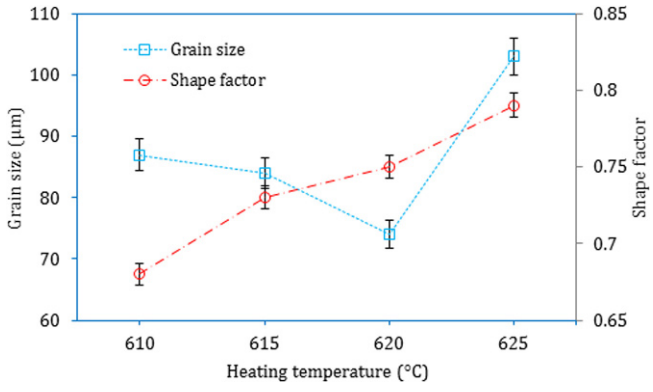


**Fig. 6.** Determined grain size and shape factor as a function of different reheating temperatures for 10 min.

gained at reheating temperature of 620 °C in which the average grain size is less than 100 μm, and the shape factor is more than 0.7. The grain size distribution histograms in different reheating temperatures also indicate the suitability of 620 °C for the semi-solid forming process (Fig. 5). As it is depicted, the grain size is almost less than 100 μm, and the grains are distributed uniformly.

### 3.3. The effect of holding time

The micrographs of the second pass PTCAP processed tubes held isothermally at a temperature of 620 °C for different periods of 5 min, 10 min, and 15 min are shown in Fig. 7. This figure indicates that a recrystallized microstructure was observed in the PTCAP-treated specimen after 5 min reheating. The microstructure has a normal polygon like morphology with respect to the diffusion of the atoms and joining with other grains [60]. It showed that 5 min reheating was enough for initial solid spheriodization while the solid particles were stuck together. Prolonging the reheating time to 10 min altered the morphology of the grains and caused separation between contacted solid particles from polygon to globular (Fig. 7(b)).

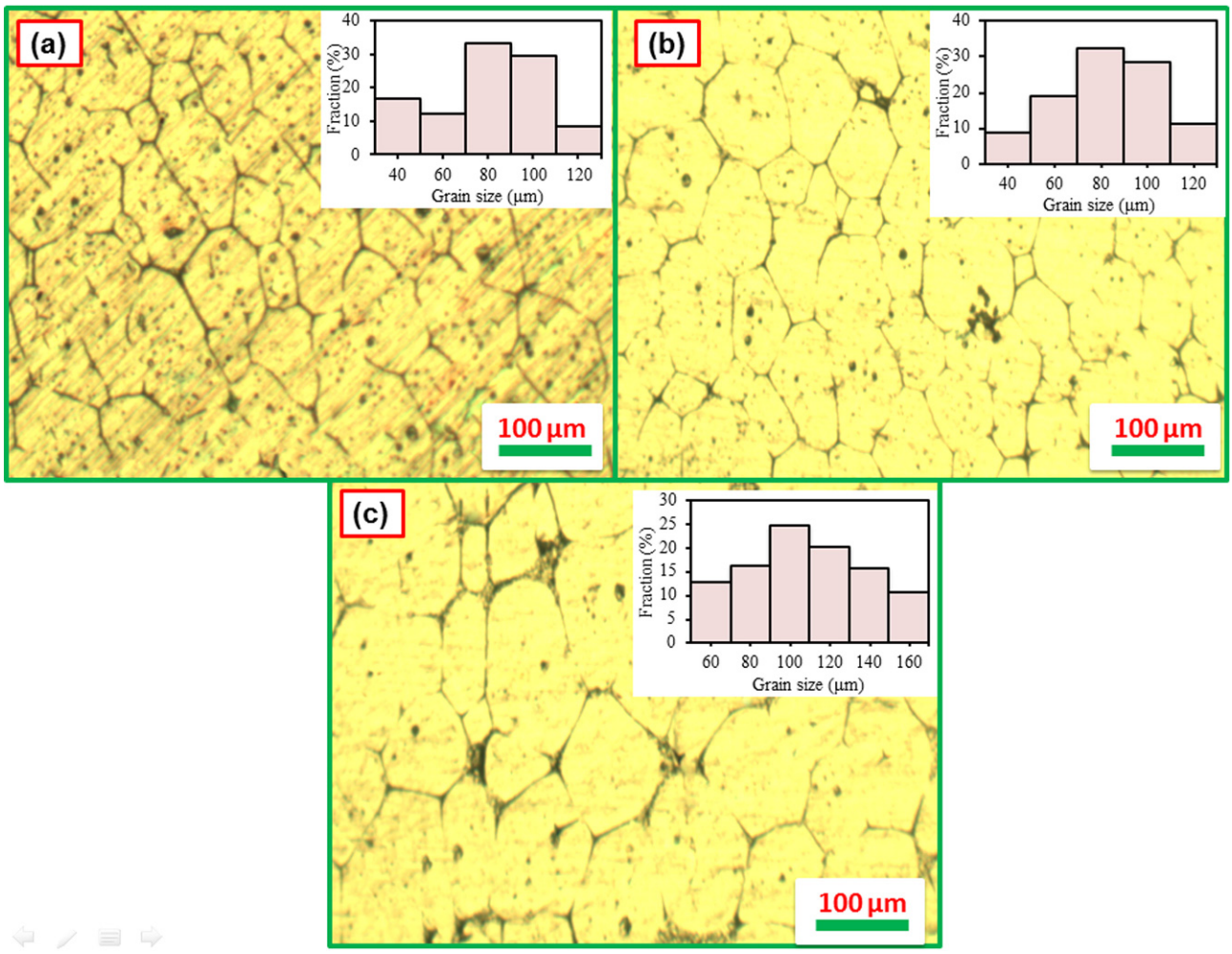


**Fig. 7.** The microstructure of the 7075 aluminum alloy tubes after two-pass PTCAP and heating at 620 °C for different times of (a) 5 min, (b) 10 min, and (c) 15 min.

In that case, a close equiaxed microstructure containing elongated and polygonal solid particles surrounded by the liquid phase at the grain boundaries could be observed. In some regions, the recrystallization phenomenon has occurred because some small grains were observed [38]. Also, when the holding time reaches 10 min, the formation of the liquid phase is observed. The formation of the liquid phase at the grain boundaries of RAP processed 7075 alloy was addressed by Atkinson *et al.* [61] because these areas retain surpassing amounts of solute concentrations [38]. Figure 7(c) indicates that longer isothermal reheating for 15 min led to a reduction in the interconnection between solid particles and a formation of coarsened globules [38].

In Fig. 7, the grain size distribution of the samples for different holding times is shown. Relevant histograms of the microstructures confirmed that the distribution of the solid particles was strongly dependent upon the holding time. The grain size became uniform as the holding time increased to 15 min. It can be seen that the grain size distribution was not uniform in a holding time of 5 min for a second pass PTCAP processed sample.

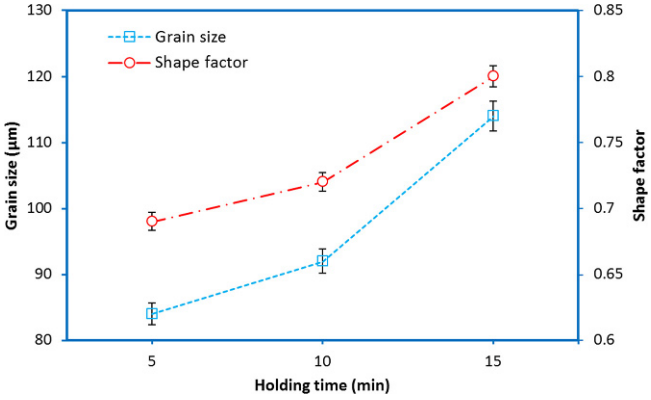


**Fig. 8.** Determined grain size and shape factor in various holding time for the 2-pass treated specimen held at 620 °C for 6 min.

The variations of both grain size and shape factor for the

PTCAP-treated specimen at different holding periods are shown in Fig. 8. It is evident that the grain size and shape factor both increased with prolonging the heating time as a consequence of decreasing the surface energy of solid particles with diminishing sharp edges [43]. Moreover, with further increases in holding times, the liquid phase between the solid particles thickens, and the liquid fraction increases. As a consequence, the Ostwald ripening mechanism can be considered as a predominant mechanism of grain coarsening [38].

To sum up, the deformation mechanism of the PTCAP-treated samples in the semi-solid zone is illustrated schematically in Fig. 9. As it is known, applying the cold working processes like PTCAP on the material increase the number and density of dislocations [47,62]. Dislocations are distributed within the matrix and create subgrain boundaries in the microstructure. When the amount of cold work (number of PTCAP passes) is more, the misorientation angle is greater and dislocations are rearranged to form new high angle grain boundaries. Finally, a balance between the dislocation creation and of their rearrangement in grain boundaries is obtained which leads to the creation of the UFG structures [47,63]. By reheating the UFG structures obtained by the severe plastic deformation, the stored strain energy is released. The sharp edges of the polygon like structure are separated gradually because of the diffusion phenomenon and then the liquid phase is formed in the recrystallized boundaries. Over time, the liquid fraction increases and Ostwald ripening mechanism is activated and finally a spherical structure containing solid particles surrounded by a liquid phase, is formed.

The microstructural features of the two-pass treated samples of A356 aluminum alloy by ECAP method [43] in the semi-solid zone are shown in Fig. 10 for a comparison with the obtained results of this study. The semi-solid temperature of the A356 and 7075 alloys were 580°C and 620°C accordingly, both with 40% of liquid fraction. As illustrated in Fig.

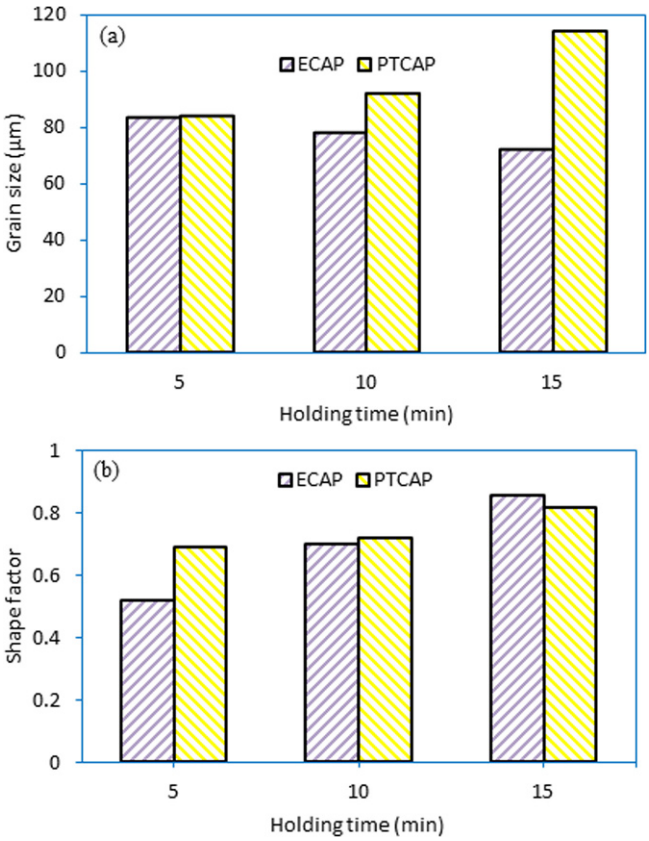


**Fig. 10.** Comparison of (a) the grain size and (b) shape factor between ECAP processed [43] and PTCAP processed Al 7075.

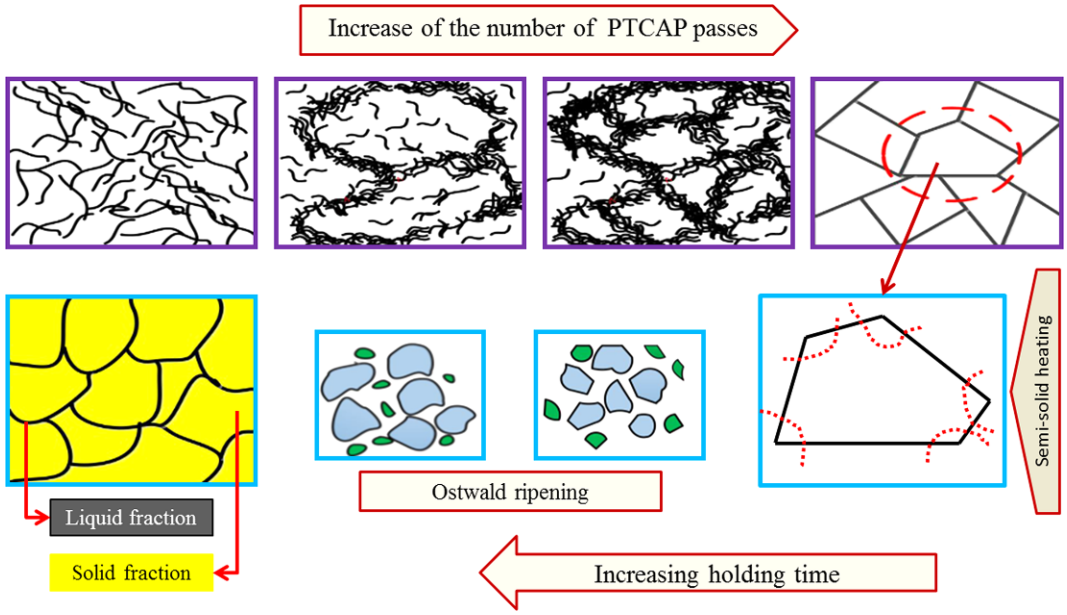


**Fig. 9.** Schematic illustration of the coarsening mechanism in PTCAP-treated samples in the semi-solid region.

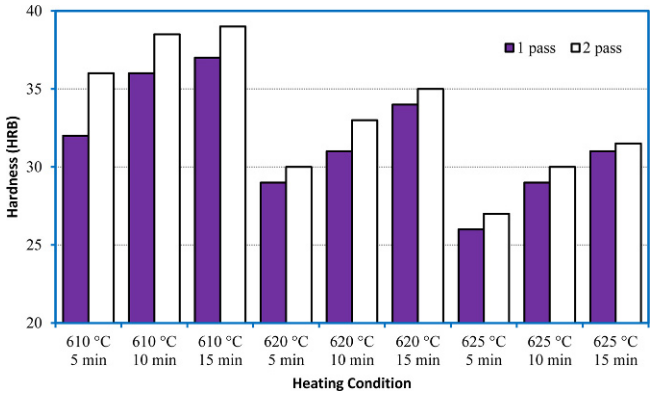


**Fig. 11.** Hardness measurements of the semi-solid samples in different heat treatment conditions.

10(a), the obtained grain size value of the two methods of applying strain stays in the desirable range of the semi-solid forming process. Moreover, the grain size of PTCAP-treated samples is somewhat larger than ECAPed ones in the semi-solid state. Also, the results indicated that the application of PTCAP process improves the shape factor only in the lower holding times while at the longer holding times were not seen significant changes in shape factor (Fig. 10(b)). These comparisons indicate the high capacity of the PTCAP process as a strain-inducing stage to obtain a suitable microstructure of semi-solid forming. This process can be widely applied in manufacturing the seamless tubes by using semi-solid forming processes.

In Fig. 11, the effect of the number of PTCAP passes, as well as the effects of reheating temperatures and times on the hardness of the alloy are shown. As it can be seen, the hardness of two-pass treated samples in different heat treatment conditions has been higher than one-pass treated ones and this phenomenon was predictable. However, as the reheating temperature and time increase, this difference becomes negligible. By increasing the reheating temperature, recrystallization of the structure continues and the stored strain energy is reduced along with the residual stresses. So, the dislocations move more easily and the hardness is decreased. On the other hand, at a specific temperature, it is observed that by increasing holding time, the hardness is increased due to the solid solution hardening phenomenon which occurs at elevated temperatures and times.

## 4. CONCLUSION

In this article, the influence of a number of PTCAP passes and semi-solid reheating on the homogeneity and microstructural characteristics of Al 7075 tubes were investigated. Accordingly, the following conclusions are obtained from the results:

(1) Increasing the number of passes from one to two change the size of grains significantly, and only minor changes can be seen in the shape factor.

(2) As the number of passes is increased, a uniform distribution can be achieved, and globulization occurs faster.

(3) As the temperature is increased, the solid particle size first decreases and then increases, while it becomes more spherical in a gradual state.

(4) The appropriate conditions for subsequent semi-solid forming processes were gained at reheating temperature of 620 °C; the average grain size was less than 100 μm, and the shape factor was more than 0.7.

(5) The suitability of 620 °C for semi-solid forming processes was confirmed by the uniform distribution of grains.

(6) The grain size and shape factor both increased along with increasing the heating time. The distribution of the solid particles was strongly dependent upon the holding time.

(7) Comparison of the grain size and shape factor between ECAP-treated and PTCAP-treated aluminum alloys in the same condition revealed a high capacity of the PTCAP process as a strain-inducing stage to achieve a suitable microstructure of semi-solid forming, especially for tube form samples.

(8) Hardness measurements showed that the two-pass PTCAP treated samples exhibited higher hardness than one-pass treated samples in all cases. Also, at a higher reheating temperature and time the difference of hardness values were negligible.

## ACKNOWLEDGEMENT

This work was supported by Iranian National Science Foundation (INSF).

## REFERENCES

1. G. Chen, Q. Chen, B. Wang, and Z.-M. Du, *Met. Mater. Int.* **21**, 897 (2015).
2. R. Meshkabadi, G. Faraji, A. Javdani, and V. Pouyafar, *T. Nonferr. Metal. Soc.* **26**, 3091 (2016).
3. J. Jayaraj, E. Fleury, K.-B. Kim, and J.-C. Lee, *Met. Mater. Int.* **11**, 257 (2005).
4. M. Flemings, R. Riek, and K. Young, *Mater. Sci. Eng.* **25**, 103 (1976).
5. D. Spencer, R. Mehrabian, and M. C. Flemings, *Metall. Trans.* **3**, 1925 (1972).
6. C. Vives, *Metall. Trans. B* **23**, 189 (1992).
7. C. Limmaneevichitr and W. Eidhed, *Mat. Sci. Eng. A* **349**, 197 (2003).
8. M. Abel-Reihim and W. Reif, *Metall* **38**, 130 (1984).
9. M. P. Kenney, J. A. Courtois, R. D. Evans, G. M. Farrior, C. P. Kyonka, K. P. Young, *et al. Metals Handbook 9th ed.*, Vol. 15, pp.327-338, ASM International, USA (1988).
10. A. Haghparast, M. Nourimotlagh, and M. Alipour, *Mater. Charact.* **71**, 6 (2012).
11. H. Jiang and M. Li, *Mater. Charact.* **54**, 451 (2005).

12. D. Kirkwood and P. Kapranos, *Met. Mater.* **5**, 16 (1989).
13. E. Tzimas, A. Zavaliangos, and A. Lawley, *Proc. 5th International Conference on Semi-Solid Processing of Alloys and Composites*, pp.345-352, Colorado School of Mines, USA (1998).
14. G. Yan, S. Zhao, S. Ma, and H. Shou, *Mater. Charact.* **69**, 45 (2012).
15. A. G. Leatham and A. Lawley, *Int. J. Powder Metall.* **29**, 321 (1993).
16. G. Faraji, M. M. Mashhadi, and H. S. Kim, *Mater. Lett.* **65**, 3009 (2011).
17. C. Xu, K. Xia, and T. G. Langdon, *Acta Mater.* **55**, 2351 (2007).
18. M. Zehetbauer, H. Stüwe, A. Vorhauer, E. Schafler, and J. Kohout, *Nanomaterials by Severe Plastic Deformation*, p. 433, Wiley, USA (2005).
19. U. Chakkingal, A. B. Suriadi, and P. Thomson, *Scripta Mater.* **39**, 677 (1998).
20. K. Edalati and Z. Horita, *J. Mater. Sci.* **45**, 4578 (2010).
21. A. Hohenwarter, *Mat. Sci. Eng. A* **626**, 80 (2015).
22. G. J. Raab, R. Z. Valiev, T. C. Lowe, and Y. T. Zhu, *Mat. Sci. Eng. A* **382**, 30 (2004).
23. D. M. Jafarlou, E. Zalnezhad, A. S. Hamouda, G. Faraji, N. A. B. Mardi, and M. A. H. Mohamed, *Metall. Mater. Trans. A* **46**, 2172 (2015).
24. G. Faraji, A. Babaei, M. M. Mashhadi, and K. Abrinia, *Mater. Lett.* **77**, 82 (2012).
25. G. Faraji and H. Kim, *Mater. Sci. Tech*. **33**, 905 (2017).
26. A. Nagasekhar, U. Chakkingal, and P. Venugopal, *J. Mater. Process. Tech.* **173**, 53 (2006).
27. H. Abdolvand, H. Sohrabi, G. Faraji, and F. Yusof, *Mater. Lett.* **143**, 167 (2015).
28. H. Torabzadeh Kashi and G. Faraji, *Modares Mech. Eng.* **16**, 271 (2016).
29. S. Hosseini, K. Abrinia, and G. Faraji, *Mater. Design* **65**, 521 (2015).
30. V. Shatermashhadi, B. Manafi, K. Abrinia, G. Faraji, and M. Sanei, *Mater. Design* **62**, 361 (2014).
31. L. Tóth, M. Arzaghi, J. Fundenberger, B. Beausir, O. Bouaziz, and R. Arruffat-Massion, *Scripta Mater.* **60**, 175 (2009).
32. J. T. Wang, Z. Li, J. Wang, and T. G. Langdon, *Scripta Mater.* **67**, 810 (2012).
33. M. Mohebbi and A. Akbarzadeh, *Mat. Sci. Eng. A* **528**, 180 (2010).
34. A. Babaei, M. Mashhadi, and H. Jafarzadeh, *Mat. Sci. Eng. A* **598**, 1 (2014).
35. A. Babaei, M. Mashhadi, and H. Jafarzadeh, *J. Mater. Sci.* **49**, 3158 (2014).
36. A. Javdani, V. Pouyafar, A. Ameli, and A. A. Volinsky, *Mater. Design* **109**, 57 (2016).
37. S. Hassas-Irani, A. Zarei-Hanzaki, B. Bazaz, and A. A. Roostaei, *Mater. Design* **46**, 579 (2013).
38. B. Binesh and M. Aghaie-Khafri, *Metals* **6**, 42 (2016).
39. H. Mohammadi, M. Ketabchi, and A. Kalaki, *Int. J. Mater. Form.* **5**, 109 (2012).
40. A. Bolouri, M. Shahmiri, and E. Cheshmeh, *T. Nonferr. Metal. Soc.* **20**, 1663 (2010).
41. A. Bolouri, M. Shahmiri, and C. Kang, *J. Alloy. Compd.* **509**, 402 (2011).
42. J. Jiang, Y. Wang, G. Xiao, and X. Nie, *J. Mater. Process. Tech.* **238**, 361 (2016).
43. S. Ashouri, M. Nili-Ahmadabadi, M. Moradi, and M. Iranpour, *J. Alloy. Compd.* **466**, 67 (2008).
44. S. H. Nedjad, H. Meidani, and M. N. Ahmadabadi, *Mat. Sci. Eng. A* **475**, 224 (2008).
45. J.-F. Jiang, L. Xin, W. Ying, J.-J. Qu, and S.-J. Luo, *T. Nonferr. Metal. Soc.* **22**, 555 (2012).
46. A. Farhoumand and R. Ebrahimi, *Mater. Design* **30**, 2152 (2009).
47. G. Faraji, M. Mashhadi, A. Bushroa, and A. Babaei, *Mat. Sci. Eng. A* **563**, 193 (2013).
48. H. Abdolvand, G. Faraji, M. B. Givi, R. Hashemi, and M. Riazat, *Met. Mater. Int.* **21**, 1068 (2015).
49. M. Afrasiab, G. Faraji, V. Tavakkoli, M. Mashhadi, and K. Dehghani, *T. Indian I. Metals* **68**, 873 (2015).
50. G. Faraji, S. Roostae, A. S. Nosrati, J. Kang, and H. Kim, *Metall. Mater. Trans. A* **46**, 1805 (2015).
51. J. Jiang, Y. Wang, J. Qu, Z. Du, Y. Sun, and S. Luo, *J. Alloy. Compd.* **497**, 62 (2010).
52. H. Mohammadi and M. Ketabchi, *Iranian J. Mat. Sci. Eng.* **10**, 155 (2013).
53. Q. Zhang, Z. Cao, Y. Zhang, G. Su, and Y. Liu, *J. Mater. Process. Tech.* **184**, 195 (2007).
54. Z. Zhao, Q. Chen, Y. Wang, and D. Shu, *Mat. Sci. Eng. A* **506**, 8 (2009).
55. M. G. Hong, J. Y. Xiang, and M. Zhang, *T. Nonferr. Metal. Soc.* **18**, 555 (2008).
56. J. Wang, H. Lin, H. Wang, and Q. Jiang, *J. Alloy. Compd.* **466**, 98 (2008).
57. S. M. Liang, R. S. Chen, and E. H. Han, *Sol. St. Phen*. **141-143**, 557 (2008).
58. E. De Freitas, E. Ferracini Jr, and M. Ferrante, *J. Mater. Process. Tech.* **146**, 241 (2004).
59. G. Hirt and R. Kopp, *Thixoforming*, p. 328, John Wiley & Sons, USA (2009).
60. Z. Wang, Z. Ji, M. Hu, and H. Xu, *Mater. Charact.* **62**, 925 (2011).
61. H. V. Atkinson, K. Burke, and G. Vaneetveld, *Mat. Sci. Eng. A* **490**, 266 (2008).
62. M. Mesbah, G. Faraji, and A. Bushroa, *Met. Mater. Int.* **22**, 288 (2016).
63. M. Mesbah, G. Faraji, and A. Bushroa, *Mat. Sci. Eng. A* **590**, 289 (2014).